Author Manuscript

Author Manuscript

Author Manuscript

Author Manuscript

HHS Public Access

Author manuscript

Ann Neurol. Author manuscript; available in PMC 2020 June 01.

Published in final edited form as:

Ann Neurol. 2019 June ; 85(6): 934–942. doi:10.1002/ana.25461.

THE "CENTRAL VEIN SIGN" IN INFLAMMATORY DEMYELINATION: THE ROLE OF FIBRILLAR COLLAGEN TYPE I

Martina Absinta, MD, PhD, **Govind Nair, PhD**, **Maria Chiara G. Monaco, PhD**, **Dragan Maric, PhD**, **Nathanael J. Lee, BS**, **Seung-Kwon Ha, DVM, PhD**, **Nicholas J. Luciano, BS**, **Pascal Sati, PhD**, **Steven Jacobson, PhD**, and **Daniel S. Reich, MD, PhD**

Translational Neuroradiology Section, National Institute of Neurological Disorders and Stroke (NINDS), National Institutes of Health (NIH), Bethesda, MD, USA

Abstract

Accumulating evidence corroborates the role of the "central vein sign" in the radiological diagnosis of multiple sclerosis (MS). Here, we report human MRI-pathological data that inflammation-dependent intracerebral remodeling of the vessel wall is directly associated with the prominence of intralesional veins on susceptibility-based MRI. In adult marmosets with experimental autoimmune encephalomyelitis (EAE), vessel-wall fibrosis was detected early in the demyelinating process, even in lesions less than two weeks old, though fibrosis was more evident after 6 weeks. Vascular remodeling consisted of both luminal enlargement and eccentric thickening of the perivascular space (fibrillar collagen type I deposition) and affected almost exclusively white matter, but not subpial cortical, lesions. The long-term effect of vessel remodeling in MS lesions is currently unknown, but it might potentially affect tissue repair.

Introduction

On susceptibility-based MRI, perivenular topography has been recently proposed to be specific to multiple sclerosis (MS)-related focal inflammatory demyelination, potentially facilitating a pathologically specific radiological diagnosis.[1, 2] This is strictly related to the fact that the immunological events triggering the formation of demyelinated lesions in the white matter (WM) typically include blood-brain-barrier (BBB) opening in small-to-medium-sized parenchymal veins and subsequent infiltration of blood-derived scavenger and demyelinating cells.[3] However, reasons for central vein conspicuity on susceptibility-based MRI, not only during the perivenular inflammatory phase at lesion onset, but also after restoration of the BBB in chronic lesions, remain unknown.

Correspondence should be addressed to: Dr. Daniel S. Reich (daniel.reich@nih.gov), Translational Neuroradiology Section/NINDS/NIH, 10 Center Drive MSC 1400, Building 10 Room 5C103, Bethesda, MD 20852, USA. Phone number: +1-301-496-1801.

Author contributions

Conception and design of the study: MA, GN, DSR. Acquisition and analysis of data: MA, GN, MCGM, DM, NJL, SKH, KJL, PS, SJ. Drafting the text and/or preparing the figures: MA, DSR.

Potential Conflicts of Interest

Dr. Daniel S. Reich received research support from collaborations with the Myelin Repair Foundation, Vertex Pharmaceuticals, and Adelson Foundation, unrelated to the present study. All the other authors report no actual or potential conflict of interest.

Author Manuscript Author Manuscript Author Manuscript Author Manuscript

Here we report MRI-neuropathological assessment of the "central vein sign"[1] in 15 supratentorial tissue blocks from 4 formalin-fixed MS brains selected based on the presence of both white matter lesions and subpial cortical demyelination. To assess the temporal evolution of venule remodeling, we also histopathologically assessed selected lesions of different ages (from acute to chronic) in 3 adult marmosets induced to have experimental autoimmune encephalomyelitis (EAE). Based on the main finding that vessel-wall fibrosis (collagen-I deposition within the perivascular space) is directly associated with the prominence of intralesional veins on susceptibility-based MRI, we further evaluated whether collagen-I might impair the morphology and differentiation of oligodendrocytes in a neural progenitor-derived oligodendrocyte culture system.

Methods

Human autopsies

All 4 MS cases (mean age 61±5 (standard deviation) years, 2 women) had longstanding, clinically progressive disease at time of death (Table 1). Causes of death were embolic brainstem stroke, infratentorial PML, and sepsis (two patients). Formalin-fixed human brains were attained at autopsy after obtaining consent from the next of kin. Brain tissue from 8 additional autopsy cases were obtained from the Human Brain Collection Core (HBCC, National Institute of Mental Health (NIMH's) Division of Intramural Research) to serve as non-neurological age-matched controls (mean 61±13 years, p=0.9, Table 2).

EAE marmosets

In 3 adult common marmosets (*Callithrix jacchus*) (2.6, 3.4, and 4 years old; 1 female), EAE had been induced, for other studies, with 0.2 mg of fresh-frozen human white matter homogenate, as previously described.[4] The age of demyelinated lesions was assessed based on their visualization on serial (approximately every other week) in vivo MRI scans.[5] The time from immunization to necropsy was 26, 282, and 134 days, respectively. After general anesthesia and transcardial perfusion with 4% paraformaldehyde (PFA), brains were removed for histopathological assessment. Animal studies were performed under a protocol approved by the Institutional Animal Care and Use Committee.

Human and marmoset neuropathology evaluation

Postmortem MRI of formalin-fixed brains included high-resolution multi-echo gradient-echo sequences at 7T MRI.[6] For each human and marmoset brain, a 3D-printed cutting box, designed based on the postmortem MRI, allowed pathological localization of radiological findings of interest.[6-8] Three- to 7-μm-thick paraffin sections were obtained from representative tissue blocks in both human (15 MS and 10 control blocks; Tables 1-2) and marmoset brains (3 whole-brain blocks). Lesion staging evaluation included staining with hematoxylin and eosin (H&E), Luxol fast blue-periodic acid-Schiff (LFB-PAS), anti-myelin proteolipid protein (PLP, MCA839G, BioRad), and anti-ionized calcium-binding adapter molecule-1 (IBA1, macrophages/microglia, #019-19741, Wako). Assessment of vascular remodeling implemented staining with Sirius Red for extracellular protein matrix (ECM), anti-collagen-IV for basement membrane (ab6586, Abcam), anti-collagen-I for fibrillar collagen (ab34710, Abcam), and anti-CD31 for vascular endothelium (ab28364, Abcam).

Author Manuscript Author Manuscript Author Manuscript Author Manuscript

Double staining used a sequential immunohistochemical (IHC) approach. Iron deposition was evaluated with DAB-Turnbull staining.[9]

Quantification was performed using an Observer 1 microscope (Zeiss, Thornwood, NY) and ImageJ/Fiji software.[10] Based on the mean wall-thickness of reference veins, such as meningeal veins or parenchymal veins in control brain tissue (24 μm (range 15–40) and 29 μm (range 20–61), respectively), a cut-off of 20 μm wall-thickness was applied to all the other MS intra- and extralesional venules. Statistical analysis was performed using Prism software v7.0b (GraphPad).

Neural progenitor-derived oligodendrocyte culture system from human fetal brain

Premyelinating oligodendrocytes were derived from primary human neural progenitor cells, as previously described.[11] Neural progenitor cells were obtained from the telencephalon of an 8-week gestation human fetal brain in accordance with NIH guidelines. To assess whether collagen-I can influence oligodendrocyte differentiation, collagen-I (#A1048301, ThermoFisher) was added to the culture medium at two different concentrations (50 μg/ml and 100 μg/ml), which, along with a collagen-free condition, were each run three times. Cells were fixed using 2% PFA at the glial-restricted precursor and premyelinating oligodendrocyte differentiation stages.[11] Cellular morphology and expression of typical markers of cellular differentiation were evaluated at each stage for each condition. The immunofluorescence protocol included anti-nestin (stem cell marker, in-house antibody),[11] anti-glial fibrillary acidic protein (GFAP, #556330, Dako), and anti-O4 (pre-oligodendrocyte marker, MAB345, EDM Millipore). Cell numbers were quantified with ImageJ/Fiji software[10] in three randomly taken fields (size 600μm × 600μm). For each condition, on bright field images, in 5 randomly taken cells, cellular ramification was quantified using fractal dimension (D) analysis[12] (ImageJ/Fiji software,[10] Fractal Box Count tool).[13] D values range from 1–1.7, where D=1 corresponds to low morphological cellular complexity and D=1.7 corresponds to high morphological complexity, as in highly ramified cells.[12, 13] Cell number, size, and ramifications were statistically analyzed using a two-way ANOVA analysis and Tukey's post-hoc comparison.

Results

Vein remodeling in chronic human MS lesions

Twenty-five prominent veins on susceptibility-based MRI were identified within 17 MS white matter lesions (Table 1). Examples of MS lesions with single or multiple prominent veins are shown in Figure 1A–C. These MRI-prominent veins were pathologically characterized by perivenular, concentric, ECM deposition (Sirius Red staining), notably collagen-I, within the perivascular space (between the endothelium and the astrocytic glia limitans; intramural collagen thickness 43±22 μm, Figure 1F). In addition, instead of appearing collapsed, the lumens of these inflammation-remodeled venules were visibly enlarged on histopathology, even relative to extralesional medium-size veins in similar areas of white matter (mean maximum transverse diameter: 210±89 and 161±54 μm, respectively, Mann-Whitney test p=0.02). In 4 of 17 lesions (3 chronic active and one chronic inactive),

Author Manuscript Author Manuscript Author Manuscript Author Manuscript

scattered iron-loaded macrophages (range 1–9, median 3) were seen within the perivascular space.

In addition to the MRI-prominent veins, we recognized several venules (range 4–24, median 5) with similar perivenular fibrosis (≥20-μm wall-thickness), especially within larger lesions. The density of veins with perivascular collagen deposition was 14-times higher in demyelinated white matter lesions than in the periplaque and 9-times higher than in control tissue (ANOVA $p<0.0001$, Figure 1E). The density of intralesional venules was not significantly different by lesion stage (chronic active, chronic inactive, remyelinated; ANOVA $p=0.3$). Only rarely was perivascular collagen deposition detected in the cortex, even in areas of subpial cortical demyelination (Figure 1D).

Temporal assessment of vein remodeling in marmoset EAE lesion development

As previously described,[4] prominent venules on T2* images can be seen also within marmoset EAE demyelinated lesions (Figure 2 A–C). Figure 2 shows vein remodeling within actively demyelinating (<2 weeks old), subacute (2–6-week-old), and chronic (>6-week-old) EAE lesions, respectively. Vein thickening and perivenular concentric ECM/collagen deposition were seen in all marmoset EAE lesions (27 venules, mean wall-thickness 13±4 μm, mean lumen transverse diameter 41±20 μm, Figure 2D–E), even in the younger active lesions (<2 weeks old). Dura mater-like intensity of Sirius Red staining was appreciated mostly in chronic EAE lesions (>6 weeks old, Figure 2C). Outside demyelinated areas, intramural collagen was found as a normal anatomical feature of the vein wall only in major cortical veins (mean wall-thickness 10±5 μm, mean lumen transverse diameter 28±11 μm, Figure 2D–E). No significant difference was found in perivascular collagen deposition and lumen diameter between intralesional venules and major cortical veins (Mann-Whitney test $p=0.08$ and $p=0.07$, respectively). For reference, the thickness of the marmoset dura mater (mean 29±11 μm) is also reported in Figure 2D.

Effect of collagen-I on neural progenitor-derived oligodendrocytes culture

In neural progenitor-derived oligodendrocyte cultures, collagen-I affected the differentiation of progenitor-derived oligodendrocytes without a clear dose-effect (Figure 3). Overall, significantly lower nuclei counts were measured after collagen-I exposure (two-way ANOVA $p=0.01$ for experimental condition; not statistically significant for differentiation stage; Figure 3). At the glial-restricted precursor stage (bipolar cells), in comparison to control, apoptosis, bizarre morphology with enlarged soma, and increased number of GFAP +/nestin- cells were noticed. At the premyelinating oligodendrocyte stage (ramified cells), in comparison to control, reduced ramification of cellular processes and increased number of GFAP+/O4- cells were seen (Figure 3). Consistent with these observations, fractal dimension analysis showed that, after collagen-I exposure, the cellular morphological complexity increased at the glial-restricted precursor stage (loss of bipolar morphology), whereas it decreased (fewer ramifications) at the premyelinating oligodendrocyte stage (two-way ANOVA $p=0.003$ for differentiation stage, $p=0.01$ for interaction between differentiation stage and experimental condition, Figure 3). Similarly, the cell size was significantly affected by collagen-I (two-way ANOVA $p=0.001$ for differentiation stage, $p=0.008$ for interaction between differentiation stage and experimental condition, Figure 3).

Author Manuscript Author Manuscript Author Manuscript Author Manuscript

Discussion

In this study, we compared the prominence on MRI of intralesional MS veins to its histopathological correlate. Even though the perivenular nature of the demyelination process in MS and relative tendency to tissue fibrosis ("sclerosis") were reported in the earliest neuropathological descriptions of the disease,[14, 15] these pathological features were not considered relevant in the diagnostic workflow until recently.[1, 2]

Under normal conditions, parenchymal veins are visible on in vivo susceptibility-based MRI due to the paramagnetism of deoxyhemoglobin, which shortens T2* relaxation. In MS, the observed MRI-prominence of intralesional veins can be further explained by both post-inflammatory enlargement of the lumen (and the related higher content of deoxyhemoglobin) and perivenular fibrillar collagen-I deposition. The latter, by increasing macromolecular content, would shorten T2/T2* decay compared to surrounding tissue, similarly to what has been widely described for other collagen-rich anatomical structures, such as tendons.[16] The relative contributions of these two factors to the MRI conspicuity of the central vein are difficult to distinguish, even at the resolution implemented in our postmortem MRI study (nominal voxel resolution 420×420×420 μm). Additionally, in some lesions, scattered iron-loaded macrophages were seen within the perivascular space, potentially contributing to vessel conspicuity on susceptibility-based MRI as well.

To address the question of the temporal onset of perivenular remodeling (i.e., whether it is an early or late pathological event in lesion development), we studied a marmoset EAE model in which demyelinated lesions are known to be perivenular[4] and in which lesion age can be precisely tracked by in vivo serial MRI after EAE induction.[5] The earliest vessel changes and collagen deposition were observed in demyelinating lesions less than 2 weeks old, but these changes were more evident after 6 weeks in chronic lesions (Figure 2). This suggests that the vein wall and perivascular space respond quickly after demyelination-inducing immunological events, and the resulting changes persist after inflammation resolves and repair commences.

Previous work suggested that astrocytes[17] and endothelial cells[18] react to the inflammatory wave at lesion onset, inducing upregulation of ECM within the perivascular space.[17,18] Perivenular collagen deposition may inhibit CCL2-dependent monocyte infiltration,[17] sealing ongoing inflammation and limiting overall lesion growth. Although we did not directly investigate the innate immune reaction, our observations here are consistent with these prior results.[17]

The long-term effect of vessel remodeling in MS lesions is unknown. It has been shown that oligodendrocyte precursor cells can migrate along vessels during brain development,[19] and it would be interesting to investigate whether, in disease, vessel fibrosis limits their ability to reach the center of demyelinated lesions and differentiate into mature oligodendrocytes. Relevantly, our findings in a neural progenitor-derived oligodendrocyte culture system[11] indicate that collagen I profoundly affects the morphology and the differentiation of both glial-restricted progenitors and premyelinating oligodendrocytes (Figure 3).

Author Manuscript Author Manuscript Author Manuscript Author Manuscript

We also noticed that, despite the cortex's high vessel density, only rarely was perivascular collagen deposition detected there, even in areas of subpial cortical demyelination (Figure 1). This is consistent with the non-perivenular topography of those lesions, which are instead linked to apposed leptomeningeal inflammation.[19] This striking difference between white matter and subpial demyelination opens further questions about the divergent reaction of the BBB to inflammation in white matter *vs.* cortex.

Perivenular collagenosis is not specific to MS and occurs in several other conditions. Collagenosis of the deep medullary veins has been recently associated with periventricular T2-hyperintensity in small vessel disease,[20] but the potential relationship of those changes to inflammation is unknown. What seems specific to MS is rather the vein's centrality in the context of demyelinated lesion formation.

In conclusion, we report MRI-pathological evidence that inflammation-dependent vascular remodeling of small-to-medium-sized veins is directly associated with the prominence of the central vein on susceptibility-based MRI. Vascular remodeling consisted of both luminal enlargement and eccentric thickening of the perivascular space (collagen deposition) and affected almost exclusively white matter, but not subpial cortical, lesions. The long-term consequences of vessel remodeling in MS lesions, and any potential impact on tissue regeneration, are currently unknown.

Acknowledgments

The Intramural Research Program of the National Institute of Neurological Disorders and Stroke supported this study. Dr. Absinta is also supported by the National Multiple Sclerosis Society (NMSS) (grant #FG 2093-A-1) and the Conrad N. Hilton Foundation (grant #17313). The Human Brain Collection Core (HBCC, National Institute of Mental Health (NIMH's) Division of Intramural Programs) provided human brain control tissue. We thank Dr. Afonso C. Silva (NIH/NINDS) for the help with marmoset EAE projects and Dr. Eugene Major (NIH/NINDS) for providing the neural progenitor cell line.

References

1. Sati P, Oh J, Constable RT, et al. The central vein sign and its clinical evaluation for the diagnosis of multiple sclerosis: a consensus statement from the North American Imaging in Multiple Sclerosis Cooperative. Nat Rev Neurol 2016;12:714–722. [PubMed: 27834394]
2. Maggi P, Absinta M, Grammatico M, et al. Central vein sign differentiates Multiple Sclerosis from central nervous system inflammatory vasculopathies. Ann Neurol 2018;83:283–294. [PubMed: 29328521]
3. Absinta M, Sati P, Reich DS. Advanced MRI and staging of multiple sclerosis lesions. Nat Rev Neurol 2016;12:358–368. [PubMed: 27125632]
4. Gaitan MI, Maggi P, Wohler J, et al. Perivenular brain lesions in a primate multiple sclerosis model at 7-tesla magnetic resonance imaging. Mult Scler 2014;20:64–71. [PubMed: 23773983]
5. Maggi P, Macri SM, Gaitan MI, et al. The formation of inflammatory demyelinated lesions in cerebral white matter. Ann Neurol 2014;76:594–608. [PubMed: 25088017]
6. Absinta M, Nair G, Filippi M, et al. Postmortem magnetic resonance imaging to guide the pathologic cut: individualized, 3-dimensionally printed cutting boxes for fixed brains. J Neuropathol Exp Neurol 2014;73:780–788. [PubMed: 25007244]
7. Guy JR, Sati P, Leibovitch E, Jacobson S, Silva AC, Reich DS. Custom fit 3D-printed brain holders for comparison of histology with MRI in marmosets. Journal of neuroscience methods 2016;257:55–63. [PubMed: 26365332]

Author Manuscript Author Manuscript Author Manuscript Author Manuscript

8. Luciano NJ, Sati P, Nair G, et al. Utilizing 3D Printing Technology to Merge MRI with Histology: A Protocol for Brain Sectioning. J Vis Exp 2016.
9. Absinta M, Sati P, Schindler M, et al. Persistent 7-tesla phase rim predicts poor outcome in new multiple sclerosis patient lesions. The Journal of clinical investigation 2016;126:2597–2609. [PubMed: 27270171]
10. Schindelin J, Arganda-Carreras I, Frise E, et al. Fiji: an open-source platform for biological-image analysis. Nat Methods 2012;9:676–682. [PubMed: 22743772]
11. Monaco MC, Maric D, Bandeian A, Leibovitch E, Yang W, Major EO. Progenitor-derived oligodendrocyte culture system from human fetal brain. J Vis Exp 2012.
12. Behar TN. Analysis of fractal dimension of O2A glial cells differentiating in vitro. Methods 2001;24:331–339. [PubMed: 11465998]
13. Lourenco T, Paes de Faria J, Bippes CA, et al. Modulation of oligodendrocyte differentiation and maturation by combined biochemical and mechanical cues. Sci Rep 2016;6:21563. [PubMed: 26879561]
14. Rindfleisch E Histologisches Detail zur grauen DegenerationvonGehirnundRuckenmark. Virchows Arch Pathol Anat Physiol Klin Med 1863;26 474–483.
15. Dawson J The histology of disseminated sclerosis. Trans R Soc Edin 1916;50:517–540.
16. LV K Mechanisms for Short T2 and T2* in Collagen-Containing Tissue. eMagRes 2012;1.
17. Mohan H, Krumbholz M, Sharma R, et al. Extracellular matrix in multiple sclerosis lesions: Fibrillar collagens, biglycan and decorin are upregulated and associated with infiltrating immune cells. Brain Pathol 2010;20:966–975. [PubMed: 20456365]
18. Zhou T, Zheng Y, Sun L, et al. Microvascular endothelial cells engulf myelin debris and promote macrophage recruitment and fibrosis after neural injury. Nature Neuroscience 2019; 22(3):421–435. [PubMed: 30664769]
19. Tsai HH, Niu J, Munji R, et al. Oligodendrocyte precursors migrate along vasculature in the developing nervous system. Science 2016;351:379–384. [PubMed: 26798014]
20. Keith J, Gao FQ, Noor R, et al. Collagenosis of the Deep Medullary Veins: An Underrecognized Pathologic Correlate of White Matter Hyperintensities and Periventricular Infarction? J Neuropathol Exp Neurol 2017;76:299–312. [PubMed: 28431180]

Author Manuscript
Author Manuscript
Author Manuscript
Author Manuscript

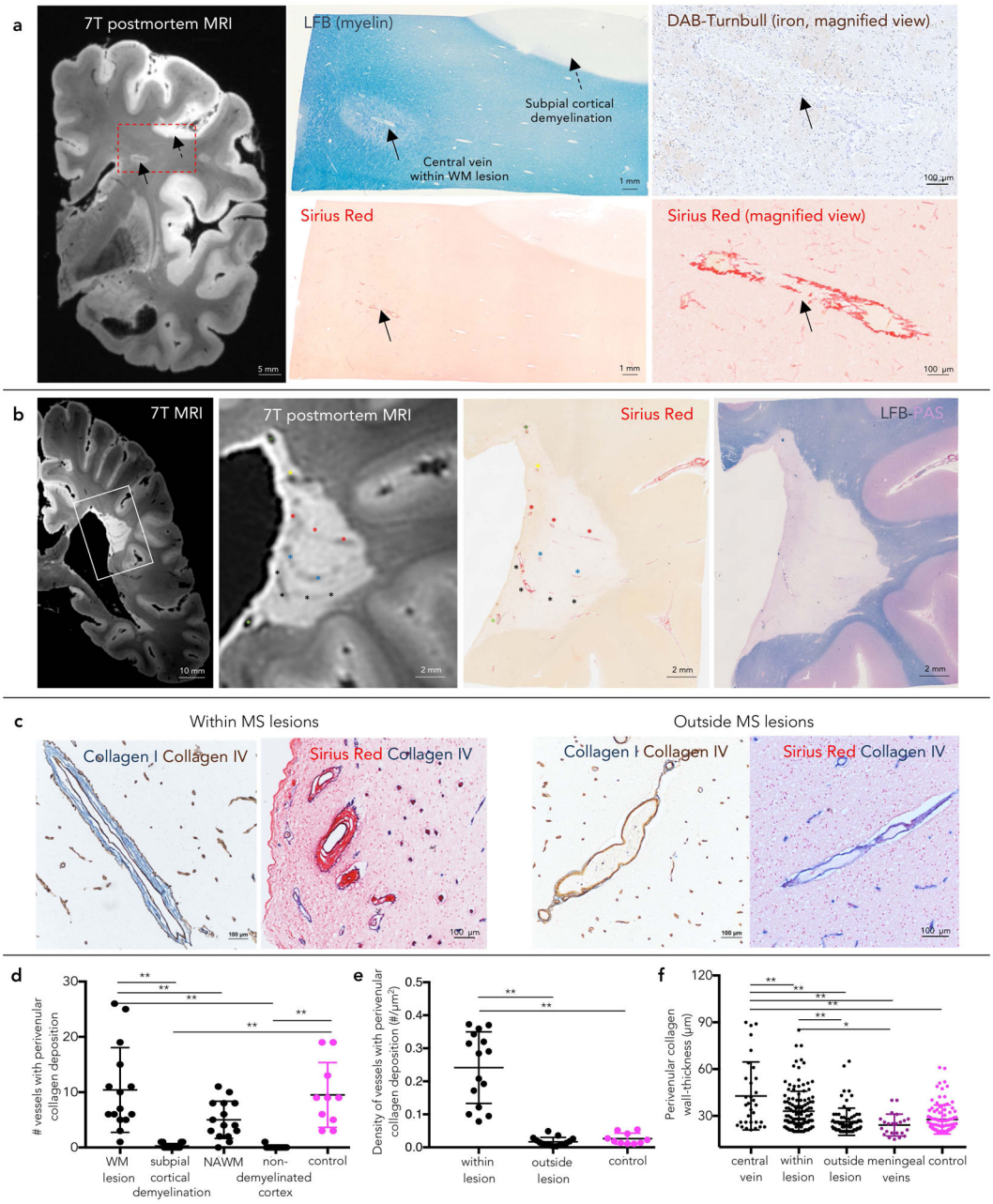

Figure 1.

Vein remodeling in chronic human MS lesions

(a) A discrete white matter lesion with a central vein on postmortem 7T MRI (gradient-echo sequence) was selected for pathological assessment (box) in a 59-year-old with progressive MS (lesion #10 in the Table 1). The prominence of the central vein is associated with luminal enlargement and extracellular matrix deposition (≥20-μm on Sirius Red staining) within the perivascular space, even in the absence of iron deposition. Veins within the subpial cortical demyelination do not show fibrosis.

(b) A periventricular demyelinated lesion (lesion #6 in the Table 1) with multiple prominent veins on postmortem 7T MRI (gradient-echo sequence). Each MRI-prominent venule shows

Author Manuscript Author Manuscript Author Manuscript Author Manuscript

venular fibrosis (Sirius Red staining). Venule trajectories are marked with colored asterisks on both magnified MRI and Sirius Red staining.

(c) Double staining for Collagen I/Collagen IV and Sirius Red/Collagen IV (basement membrane) in a 68-year-old with progressive MS (case #2). Within MS lesions, concentric deposition of fibrillar collagen I is seen within the perivascular space in both small and medium-sized parenchymal veins. Within the normal-appearing WM, veins devoid of prominent intramural fibrosis are shown as reference.

(d–e) Quantification (mean and standard deviation) of absolute number and density of veins with perivenular collagen deposition (≥20-μm-thickness) at different locations and in control tissue (ANOVA <0.0001 and <0.0001, respectively, post-hoc comparison; **p<0.001).

(f) Quantification (mean and standard deviation) of the collagen wall-thickness of veins at different locations and in control tissue (ANOVA <0.0001, respectively, post-hoc comparison ** p<0.001, *p<0.01). On average, central veins show higher collagen wall-thickness than any other analyzed veins.

Abbreviations: WM: white matter; NAWM: normal appearing white matter by MRI.

Author Manuscript Author Manuscript Author Manuscript Author Manuscript

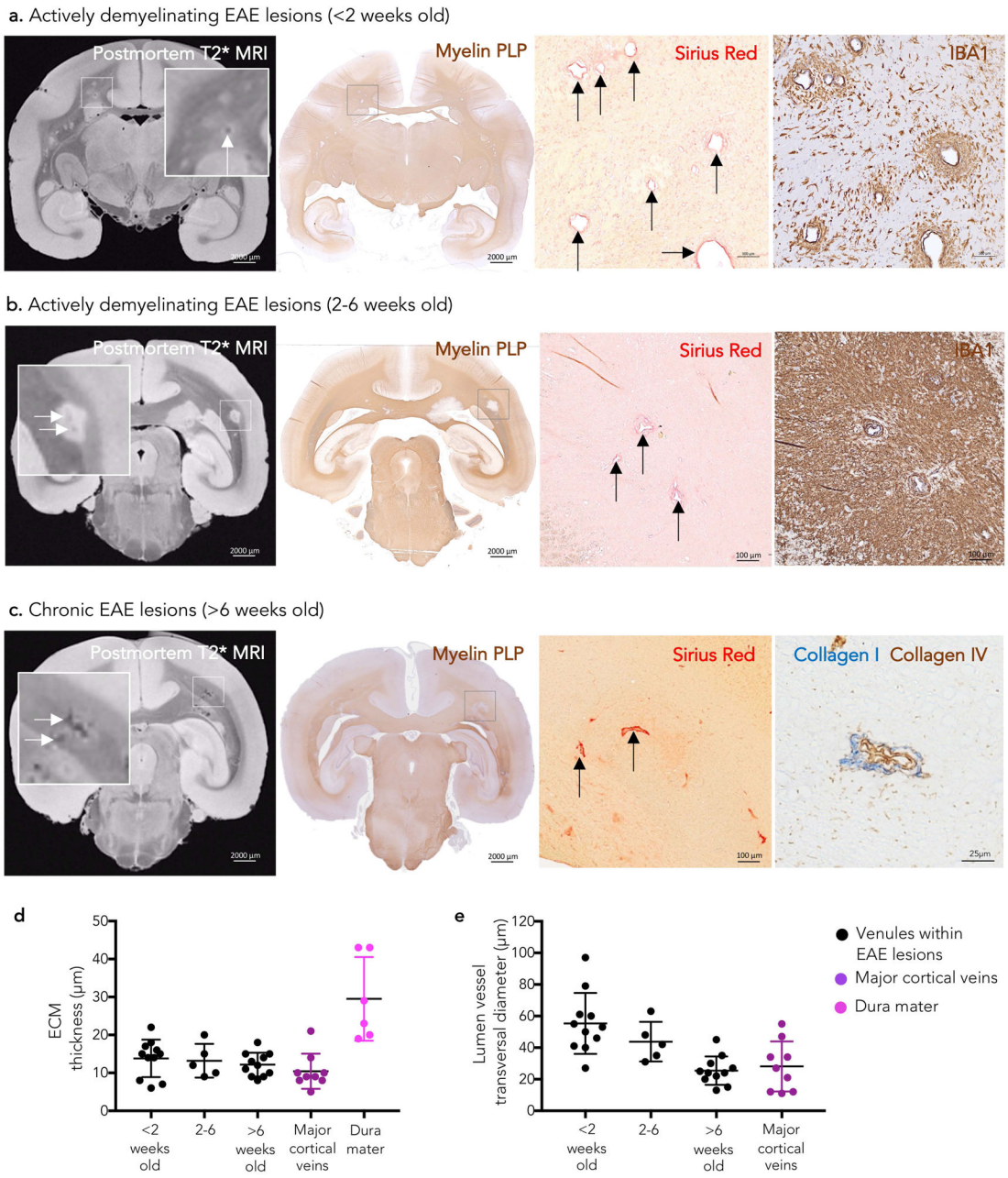

Figure 2.

MRI-pathology of venular remodeling in marmoset EAE lesion development Venular remodeling is seen early in marmoset EAE lesion development on both postmortem T2* MRI (white arrows) and histopathology. Magnified views of lesions with remodeled blood vessels (black arrows) are shown in the boxes.

(a) In lesions younger than 2 weeks, demyelination (myelin PLP) and inflammatory infiltrate (IBA1) are limited to the perivenular parenchyma.

(b) In lesions between 2 and 6 weeks old, both demyelination and inflammatory infiltrate are more extensive.

Author Manuscript Author Manuscript Author Manuscript Author Manuscript

(c) Small demyelinated lesions older than 6 weeks (chronic) show prominent perivenular extracellular matrix deposition. Double staining of a representative venule for collagen IV (basement membrane, brown) and fibrillary collagen I (blue) from the same animal (non-contiguous paraffin section).
(d-e) Quantification (mean and standard deviation) of perivascular wall-thickness and lumen vessel transversal maximum diameter of venules within EAE lesions and major cortical veins showing ECM deposition. Remodeled venules within marmoset EAE lesions resemble major cortical veins in terms of size and presence of collagen perivascular deposition. See the text for statistical analysis.
Abbreviations: EAE: experimental autoimmune encephalomyelitis; myelin PLP: myelin proteolipid protein; ECM: extracellular matrix.

Author Manuscript Author Manuscript Author Manuscript Author Manuscript

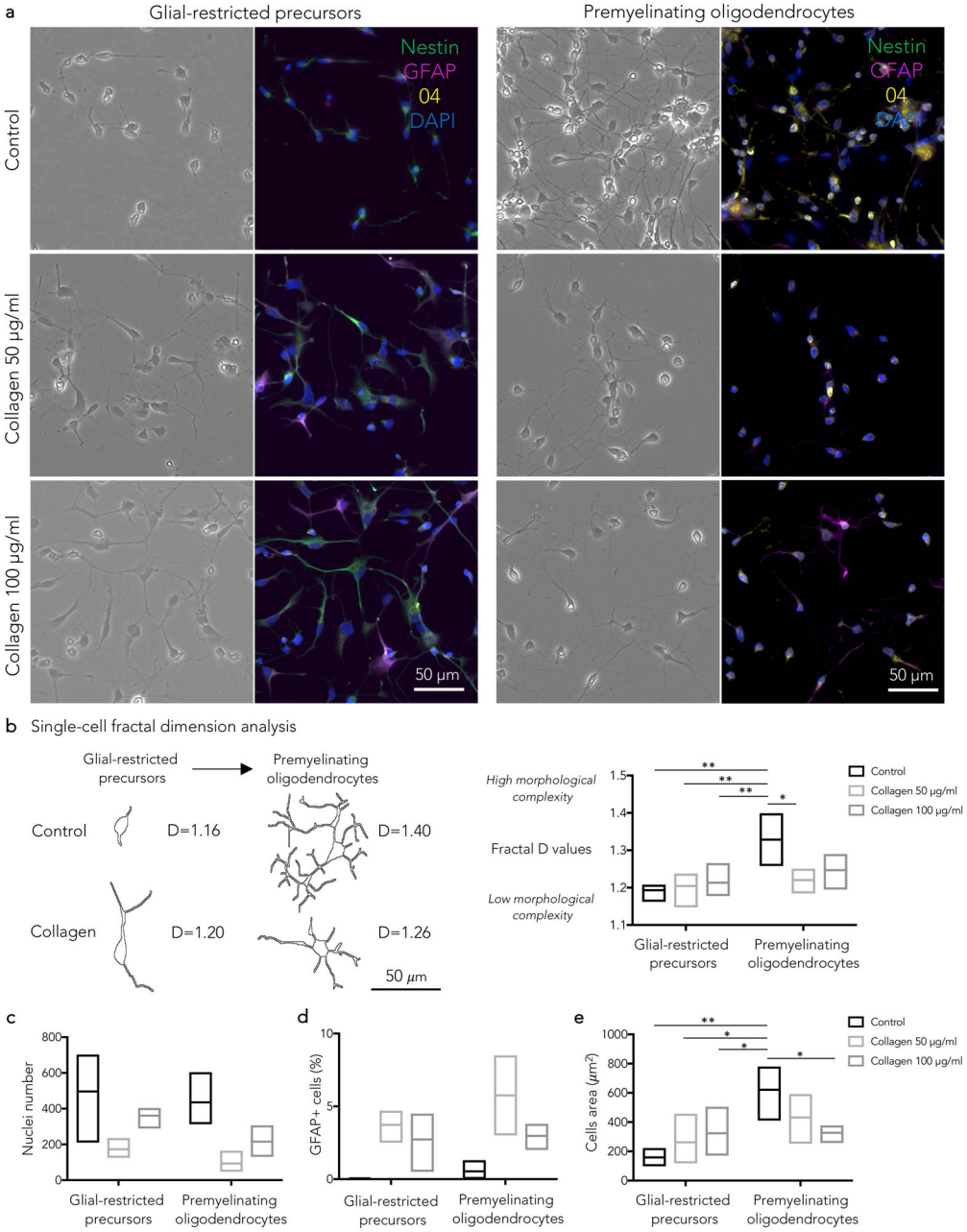

Figure 3.

(a) Phase contrast microscopy and immunofluorescence staining of glial-restricted progenitors (grown in oligomedium and specific growth factors for 2 weeks) and premyelinating oligodendrocytes (5 days after withdrawal of 4 growth factors: Shh, NT-3, bFGF, and PDGF-AA). Three experimental conditions were evaluated (control, collagen 50 µg/ml, and collagen 100 µg/ml). For neural progenitor-derived oligodendrocytes culture system protocol details see Monaco et al., J. Vis. Exp 2012.[11]

- Glial-restricted precursors: in comparison to control, collagen I induced apoptosis (fragmented or pyknotic nuclei), bizarre cellular morphology (enlarged

Author Manuscript Author Manuscript Author Manuscript Author Manuscript

soma, loss of bipolar morphology, thick processes) and increased number of GFAP+/nestin- cells (b,c,d,e).

- Premyelinating oligodendrocytes: in comparison to control, collagen I induced lower cell counts (c), reduced ramification of cellular processes (b) and increased number of GFAP+/O4- cells (d).

(b) Single-cell fractal dimension (D) analysis. Representative cells at different differentiation stages, selected for the fractal dimension analysis, are shown with corresponding D values. D values quantify the degree of cellular morphological complexity (low in bipolar cells, high in ramified cells).
See the text for statistical analysis; Tukey's post-hoc comparison *p<0.05; **p<0.01

Author Manuscript Author Manuscript Author Manuscript Author Manuscript

Table 1.

Human pathology: multiple sclerosis cases

Case	Clinical data	Block #	Lesion	Lesion pathological stage	Lesion max diameter/ area*	# MRI-prominent central veins
1	59-year-old man with progressive MS (EDSS 6.5; disease duration: 21 years; untreated at time of death; cause of death: embolic brainstem stroke; PMI: 9 hours)	1	1 frontal periventricular	Chronic active/slowly expanding	11.6 mm/52.7 mm^2	1
		2	2 frontal periventricular partially confluent lesions	Chronic active/slowly expanding	9.5 mm/49.4 mm^2 and 6.6 mm/20.5 mm^2	2
		3	1 occipital leukocortical	Chronic active/slowly expanding	9.4 mm/30.6 mm^2	2
		4	1 leukocortical occipital	Chronic active/slowly expanding	13.4 mm/81.3 mm^2	2
		5	1 frontal WM	Chronic active/slowly expanding	8.5 mm/35.0 mm^2	1
		6	1 parieto-occipital periventricular	Chronic active/slowly expanding	10 mm/51.5 mm^2	4
2	68-year-old woman with progressive MS (EDSS 7.5; disease duration: 20 years; on treatment with natalizumab; cause of death: infratentorial PML; PMI: 19 hours)	7	1 frontal periventricular	Chronic inactive	11.3 mm/110.5 mm^2	3
		8	1 parietal periventricular	Chronic inactive	7.0 mm/40.5 mm^2	2
3	60-years-old man with progressive MS (EDSS 7.5; disease duration: 16 years; on treatment with natalizumab; cause of death: sepsis; PMI: 7hours)	9	1 occipital WM	Chronic inactive	5.3 mm/16.1 mm^2	1
		10	1 frontal WM	Remyelinated/ Shadow plaque	3.1 mm/5.2 mm^2	1
		11	1 frontal periventricular	Remyelinated/ Shadow plaque	5.9 mm/17.5 mm^2	1
		12	1 frontal periventricular	Chronic inactive	7.8 mm/24.7 mm^2	1
		13	1 frontal WM	Remyelinated/ Shadow plaque	3.6 mm/17.2 mm^2	1
4	68-year-old woman with progressive MS (EDSS 7; disease duration: 30 years; untreated at time of death; cause of death: sepsis; PMI: 89 hours)	14	1 parietal periventricular	Chronic inactive	11.7 mm/87.9 mm^2	1
		15	2 frontal lesions	Chronic inactive	5.6 mm/12.5 $mm^2$and 6.2 mm/ 16.3 mm^2	2

Abbreviations: MS=multiple sclerosis, WM=white matter; PMI=post-mortem interval.

* Lesion maximum diameter and area were measured on LFB or PLP myelin staining. In leukocortical lesions, lesion area refers only to WM demyelinated area.

Author Manuscript

Author Manuscript

Author Manuscript

Author Manuscript

Table 2.

Human pathology: control cases

Case	Clinical data	Tissue block	Location
1	58-year-old woman with systemic sarcoidosis (PMI: 24 hours)	1	Medial temporal lobe/Basal ganglia
2	66-years-old man with hypertensive, atherosclerotic, and valvular cardiovascular disease (PMI: 33 hours)	2	Medial temporal lobe/Basal ganglia
3	65-year-old woman with acute pulmonary thromboemboli; hypertensive and arteriosclerotic cardiovascular disease (PMI: 28 hours)	3	Medial temporal lobe/Basal ganglia
4	63-year-old man with hypertensive cardiovascular disease (PMI: 49 hours)	4	Medial temporal lobe/Basal ganglia
5	84-year-old man with multiple impact injuries (PMI: 27 hours)	5	Medial temporal lobe/Basal ganglia
6	50-year-old man with atherosclerotic cardiovascular disease (PMI: unknown)	6	Frontal lobe
7	40-year-old woman with multiple impact injuries (PMI: unknown)	7	Frontal lobe
		8	Parietal lobe
8	64-year-old man with atherosclerotic cardiovascular disease (PMI: unknown)	9	Frontal lobe
		10	Parietal lobe

Abbreviations: PMI=post-mortem interval.